The transfer of wind waves from the shelf to the coastal zone (*)

M. SCLAVO (**) and L. CAVALERI
Istituto Studio Dinamica Grandi Masse, S. Polo 1364, 30125 Venice, Italy

(ricevuto il 10 Gennaio 2000, approvato il 31 Marzo 2000)

Summary. — We analyse and discuss the main processes that affect the characteristics of wind waves while these move through the coastal zone, towards the shore. The focus is on the influence of each process on the final results and on the overall accuracy. To this aim we make full use of two large data sets collected at different locations. Model and measured data are repeatedly compared, providing evidence of the relevance of the different processes.

PACS 92.10 – Physics of the oceans.
PACS 92.10.Hm – Surface waves, Tides, and sea level.

1. – The structure of the paper

This paper focuses on the modelling of wind waves when they enter the shallow-water coastal zone and approach the shore. In this area changes can take place within rather limited distances, and a good physical perception of the relevance of the various physical processes is a necessary prerequisite for a proper use of the numerical tool represented by the model. Such a perception can only be acquired using the model for cases where sufficiently varied measured data are available to carry out a throughout comparison. The tests here described have been carried out using two large data sets obtained at two different locations.

In the next section we briefly describe the wave model used for the tests, while in sect. **3** we describe the areas of the measurement campaigns and the available data. The results are reported in sects. **4** and **5**, while sect. **6** is devoted to a discussion of the overall findings.

2. – Numerical modelling

For the present tests we have made use of Swan, an advanced third-generation model, specifically developed for shallow-water applications, available in public domain.

(*) The authors of this paper have agreed to not receive the proofs for correction.
(**) E-mail: sclavo@flux.isdgm.ve.cnr.it

Swan takes into full consideration all the dominant physical processes that control the evolution of the wave field. In particular Swan includes a computation of the nonlinear wave-wave interactions. both in deep (quadruplets) and shallow water (triads). A full description of the model is provided by Holthuijsen *et al.* (1993), Booij *et al.* (1999), and Ris *et al.* (1999).

Swan has been run with 25 frequencies and 24 uniformely distributed directions. The frequecies are geometrically distributed, with $f_{n+1} = 1.1 f_n$ and $f_1 = 0.04$ Hz. The model has been run in stationary mode, *i.e.* given the input wave conditions at the outer border, the model iterates till when equilibrium conditions have been reached. This has been allowed by the relatively limited extent of the areas under study (see next section) and the consequent limited time required for the waves to move throughout the grid.

Full freedom exists about the choice of the grid, both for resolution and orientation. However, as further discussed in sect. **5**, the results can be very sensitive to the choice, particularly with respect to that of the boundary conditions.

Swan is freely available from Delft Technological University, at: http://swan.ct.tudelft.nl.

3. – The available data

For our present purposes we make use of the data obtained from two measurement campaigns, carried out, respectively, at Holderness and Montalto di Castro.

Holderness (see fig. 1) is located on the East coast of England. The experiment (see

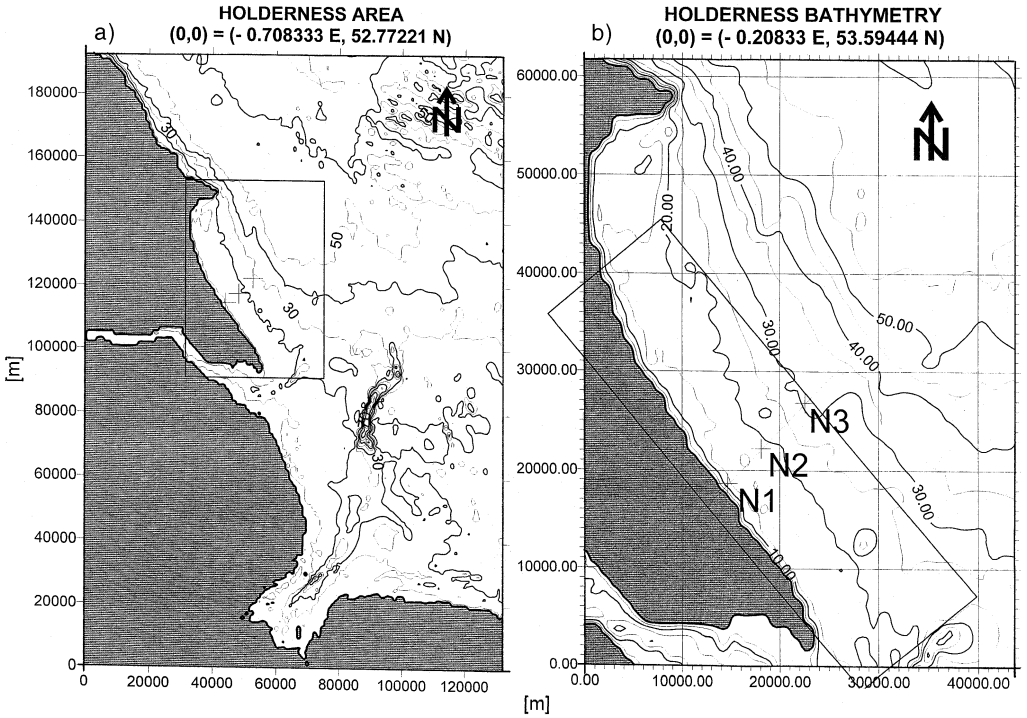

Fig. 1. – a) General view of the Holderness area, on the East coast of England. b) Enlarged section: locations N1, N2, N3 of the buoys and position of the computational grid. The isobaths and the coordinates are in metres (after Sclavo and Cavaleri, 1999).

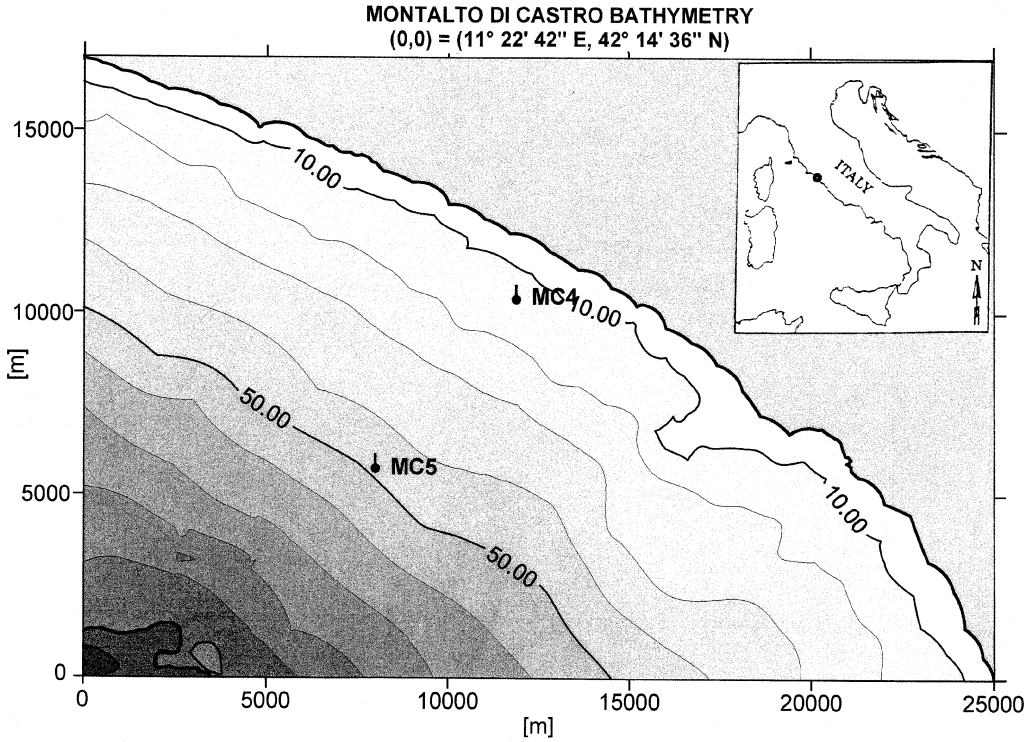

Fig. 2. – The bathymetry off the coast at Montalto di Castro, on the west coast of Italy (see the small frame for the location). Isobaths in metres. MC4 and MC5 mark the positions of the two wave measuring buoys, the offshore one with directional properties.

Prandle *et al.*, 1996) aimed at monitoring the erosion of the local cliffs and it lasted two winters, during which three wave measuring buoys were moored at different depths (12, 18, 30 metres) and different distances from the coast (1, 6, 12 km). The two offshore buoys provided also directional information, allowing a fully specified input at the border of the local grid. In the area the isobaths are more or less parallel to the coast. The bottom is a mixture of sand and mud, with median grain size D_{50} of about 1.5 mm.

Montalto di Castro (see fig. 2) is located on the West coast of Italy, on the Tyrrhenian Sea. The overall geometry is similar to Holderness, with the isobaths basically parallel to the shoreline. Two buoys, the offshore one with directional properties, were moored at 7.5 and 1.5 km from the coast, on a depth of, respectively, 50 and 15 metres. The measurements are part of the monitoring campaign done by ENEL, the Italian National Electricity Company.

Of the many possible results, we focus here on the significant wave height H_s, typically comparing model and measured values at the inshore buoy. Also, out of the many physical processes that can affect the wave conditions close to the coast, we report on those that are relevant in the two quoted campaigns and turn out to be so for most of the practical cases.

4. – Results from the Holderness dataset

The grid for the Holderness area was set as in fig. 1, *i.e.* with the longest axis parallel to the shore and intersecting the location of the offshore buoys, whose data have been taken as boundary conditions, uniform all along the external border. Null conditions were assumed on the sides of the grid (perpendicular to the shoreline). To do this, the grid has been chosen large enough to exclude any influence from the sides of the central zone, where the buoys were located. The resolution was fixed at 1 km, with consequent 16×51 dimensions of the grid.

Out of the large number of records available, we have selected the ones with a wave height (at the offshore buoy) larger than 0.5 m. The peak incoming direction θ_p (degrees, clockwise with respect to North) was required to be between 20° and 80°, *i.e.* within a 60 degrees sector centered on the perpendicular to the shore.

The overall result with the default option of the Swan model is shown in fig. 3, where we compare the model results (vertical scale) *vs.* the buoy data (horizontal scale). Each mark corresponds to a single record, hence a run of the model. With the set-up mentioned in sect. **2** (25 frequencies and 24 directions), one run of the model requires ten seconds on a Pentium II 400 MHz. On the average the system converges to the final solution within 3 or 4 iterations.

Looking at fig. 3a, and being these the boundary conditions derived from the buoy data, we should expect a perfect fit between model and measured data, *i.e.* all the marks to be on the 45° diagonal line. The discrepancy, to be discussed later, derives from considering in the model the wave components propagating in the 60 degree sector specified above.

We discuss now the single processes relevant for these cases.

4·1. *Bottom friction.* – From fig. 3c we see that the model overestimates the wave height at N1, *i.e.* it underestimates the energy loss while moving from N3 to N1. In these conditions, and before entering the surf-zone, the dominant process is usually bottom friction. We note that the default value for the bottom friction coefficient, following Collins (1972), has been taken equal to 0.015. However, this value is typical of very fine sand, while the relatively coarse one at Holderness leads to a larger dissipation. Following Sleath (1984), we take the friction factor $c_f = 0.040$. This, see fig. 4, clearly improves the results, the overestimate at N1 being now limited to 8%.

With a further tuning of c_f it would be possible to reach an almost perfect fit between model results and measured data. However, such a tuning would have a purely local value. When moving to a different area, with a different bottom material, a completely different calibration would be required. The main message, and this was the reason for the tests, is that, till when the bottom induced breaking takes over in the surf-zone, the wave conditions in shallow water are dominated by bottom friction. Its correct representation in the model is therefore crucial for the quality of the results. Because c_f depends on the grain size, we cannot rely on default values, and a reasoned choice, based on information on the grain size of the area of interest, is required.

The problem is further complicated because c_f is also a function of the geometrical characteristics of the bottom (smooth, rippled, etc.), which depend in turn on the actual wave conditions. The associated variability, that we have not taken into account, can help to explain (together with the accuracy and confidence limits of the measurements and other approximations in the Swan model) the scatter of the results around the best fit lines in fig. 3 and fig. 4.

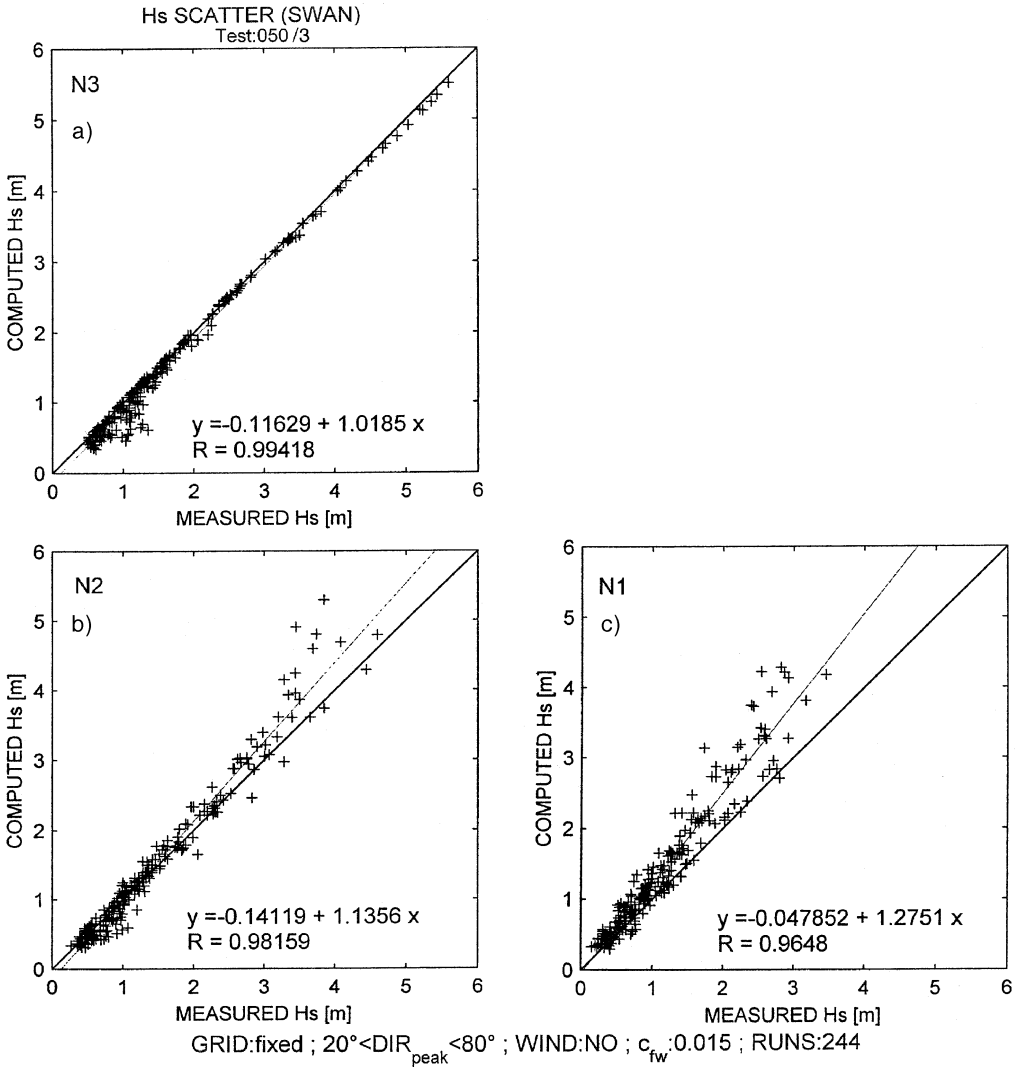

Fig. 3. – Computed significant wave height H_s at N3, N2, and N1 (see fig. 1b for their location) with respect to the measured values. For these runs the bottom friction factor c_f was set at 0.015, model default option (after Sclavo and Cavaleri, 1999).

4·2. *White capping and generation by wind.* – Wind is the basic source of energy for the waves we are presently interested in, and it is natural to take it into consideration while modelling the evolution of the wave field close to the coast. However, we must realize that the spatial scale involved in the generation of high waves can be very large, up to one thousand kilometres or more. Therefore, if the area we are looking at is relatively small, *e.g.* less than 20–30 km, the net effect of the wind is likely to be quite limited.

We have used the word "net" on purpose. The actual amount of energy transfered from wind to waves is not small at all, but most of it is immediately lost by white

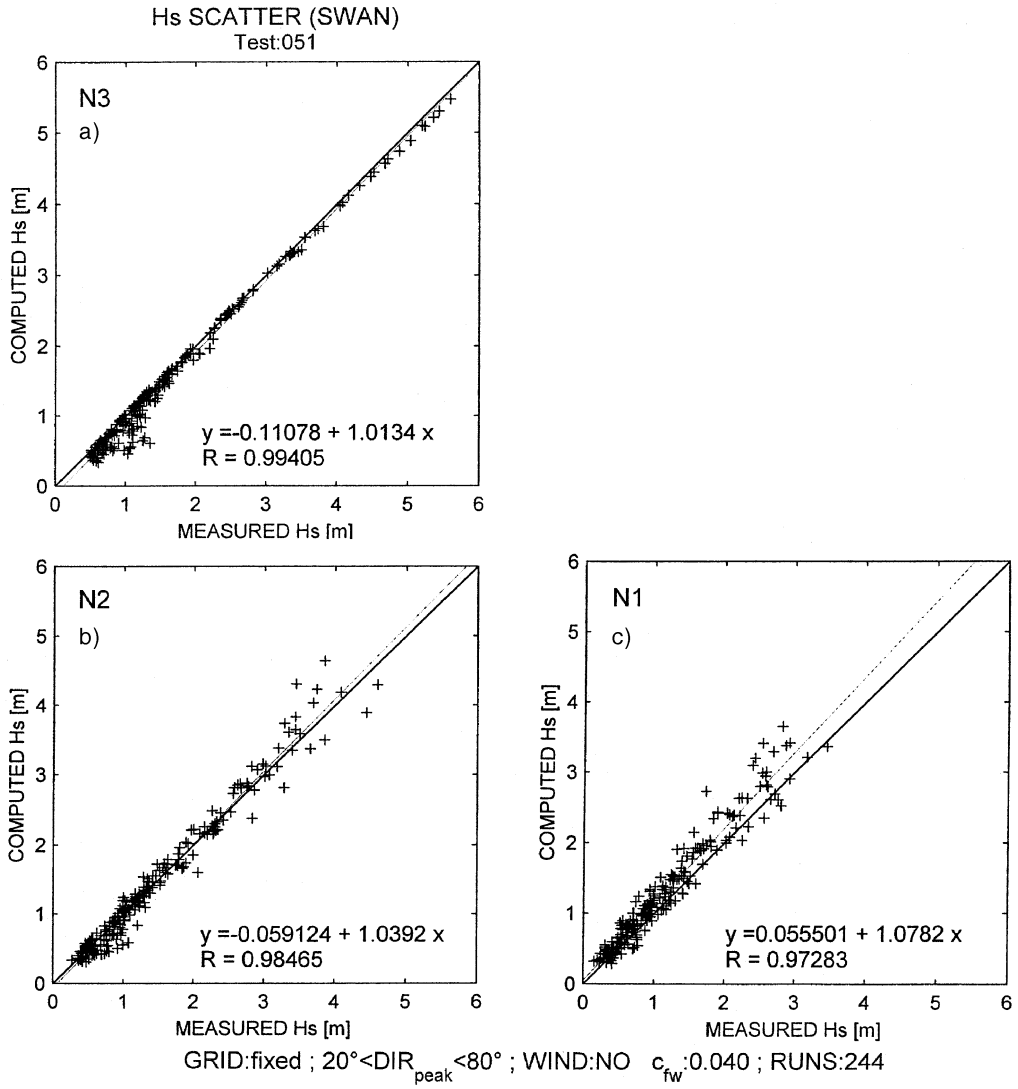

Fig. 4. – As fig. 3, but with the bottom friction coefficient increased to $c_f = 0.040$ (after Sclavo and Cavaleri, 1999).

capping and transfered to turbulence and general circulation (see Komen *et al.*, 1994). Typically only 10% is retained into the wave field, which is why the wave growth is a relatively slow process.

An implication of this is that it is not physically sound to switch off in the model only either the generation by wind or the white capping. The latter one is strictly associated to the process of generation, and therefore to the wind.

In the case of Holderness the limited spatial scale implies a small influence by wind on the results. This is indeed the case. For the tests we have used the analysis

wind produced by the European Centre for Medium-Range Weather Forecasts (ECMWF, Reading, U.K.).

The results show an influence by wind that is in general limited to a few percents. The only case when it becomes relevant is when the waves are locally generated. It is up to the user to decide if they are of interest for his specific purposes.

4·3. *Nonlinear interactions.* – When certain resonance conditions are verified, wave components exchange energy among themselves. Being conservative, the process does not affect directly the overall energy budget. However, it does affect the energy distribution within the spectrum, and therefore all the processes directly connected to it.

In deep water the resonance occur within quadruplets of wave components that satisfy certain resonance conditions on their frequencies and wave numbers. Because of the time scale involved, in general it is not necessary to consider these nonlinear interactions for the evolution of the wave field close to the coast. However, the conditions for resonance change in shallow water. Because of the different dispersion relationship, here the resonance takes place also between triplets of wave components. Also because of the higher steepness of waves in shallow waters, the rate of exchange is highly enhanced, and macroscopic changes do occur within a short distance. The so-called third-order nonlinear wave-wave interactions, or triads (see, *e.g.*, Ris *et al.*, 1998), are responsible, among other things, for the appearance of spectral peaks at frequencies multiple of the dominant one.

In the case of Holderness the triads were switched off in the model to check their influence on the results. There was virtually no change. The point to be remembered is that the effect of the triads increases dramatically with decreasing depth. In normal conditions, with wave period smaller than 10–12 s, they becomes relevant only on a depth of a few metres, which was not the case at Holderness.

4·4. *Spectral/parametric input.* – As previously mentioned, Swan is a fully spectral model. In principle, a full two-dimensional spectrum $E(f, \theta)$ is required as input information at the boundary. When a 2D spectrum is not available, a best guess is done, deriving the 2D information from the available one.

In the case of the Holderness dataset we are in relatively favourable conditions, because the offshore buoy is a directional one, and therefore we have enough information (mean direction and spread for each frequency) to build a reliable 2D spectrum as boundary conditions. However, in most practical cases the only information available offshore is parametric, *i.e.* only the integrated parameters H_s, T_m or T_p (mean or peak period), θ_m or θ_p (mean or peak direction) are available. This leads to further uncertainty on the input conditions, hence on the results at the coast.

To explore the sensitivity of the results to the above point, we have carried out a series of tests, comparing the output at the coast, N1 in our case, as derived first with a spectral, then with a parametric approach. More specifically, we have selected from the Holderness dataset all the cases with an incoming θ_m within a 150 degree sector centered on the perpendicular to the shore. As in the previous series of tests, H_s at the offshore buoy was required to be larger than 0.5 m. This left us with 812 cases that were first run making full use of the information available at N3 (spectral approach). Then we derived H_s, T_m, θ_m at N3, and fed the model with this condensed information, exploding for each single run the triplet into a Jonswap spectrum. The

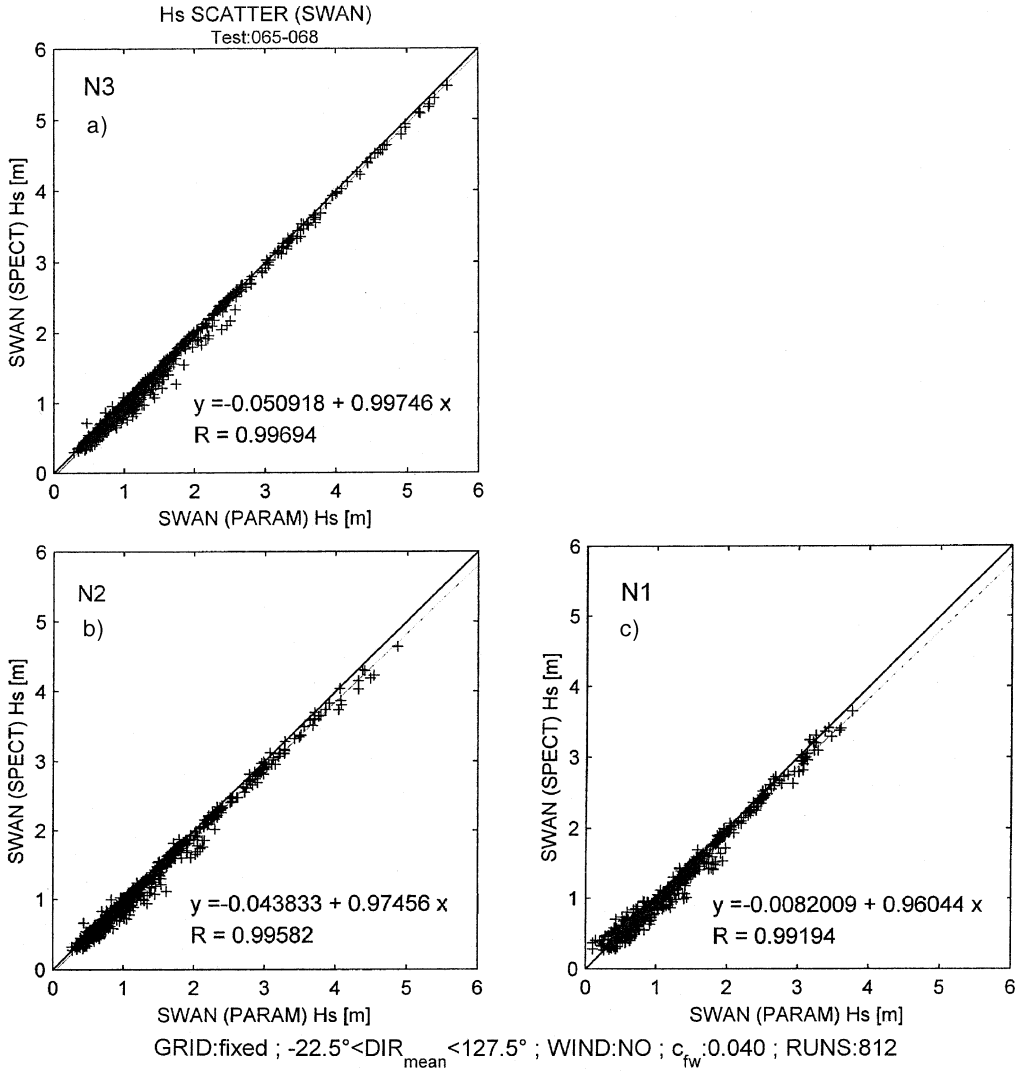

Fig. 5. – Significant wave height H_s at N3, N2 and N1 (see fig. 1b for their location) computed with a spectral input (vertical) with respect to the values obtained with a parametric input (horizontal). For these runs the bottom friction factor c_f was 0.040.

approximation is clearly given by the differences between the two input spectra. The results of the tests are shown in fig. 5, where we compare at each of the three buoys the spectral and the parametric results.

The first thing to note is the presence of several cases at N3 where the spectral input H_s is lower than the parametric one. The explanation, which holds also for the panel a) of fig. 3, is that in the parametric runs all the wave components, whichever their direction, are summarized into a single value θ_m, around which the 2D spectrum is exploded. In the case of an offshore blowing wind we can have locally generated wind waves superimposed to a dominant incoming swell. If working with a parametric

approach, all this energy appears to the model as distributed around the mean direction θ_m, expectably very similar to that of the incoming swell. However, the wind is still present, and the model reacts generating a new offshore going wave system, with the result of an increased model H_s at the offshore buoy.

The central and right panels in fig. 5 are a mere consequence of the distribution in panel a), showing that the parametric approach generally gives higher results. However, the differences are limited to a few percents. The overall conclusion is that, if we are interested only in the integrated parameters, and at least in conditions similar to the ones present at Holderness, quite acceptable results at the coast can be obtained also when the information available offshore is limited to the integrated parameters H_s, T and θ.

If this is enough it depends on the use we are going to make of the results. If a detailed spectral description is required, a parametric approach can be defective. However, in many cases this is what we have, and we have to live with it. In these cases it is worthwhile to be aware of the possible errors involved in the approximation. A few runs with a numerical model, similar to the one we have described, will be very useful to understand the limitations of the parametric approach.

4·5. *Statistics.* – Directly connected to the differences between spectral and parametric approaches are also the implications for long term statistics. A common application of a time series of offshore wave data is the derivation of the corresponding statistics at a nearby coastal location. Figure 6 summarizes the possible approaches to the problem, depending on the data we have at disposal. The associated numerical example concerns the Holderness data, but the scheme is quite general.

We start from the offshore spectra (the 1D SPECTRA just above the centre of the figure), clearly the best and most complete information. For the transport to the coast we usually select only the cases where the mean direction θ_m is directed, within a certain angle, towards the shore (for Holderness this implies $337° < \theta_m < 127°$). Then we use the spectra as input to local modelling (Swan in the present case), we evaluate the spectra at the coast or nearby, then the local integrated parameters (T.S. = time series), from which we get an estimate of the local statistics. Granted the accuracy of the model, this is our best estimate, C, of the wave climate at our target location (N1 or N2 in the case of Holderness).

Let us now see the alternative procedure. Rather than the spectra, it is common to have at disposal time series of the integrated parameters (T.S. "A", second column from the left in fig. 6). With the same filtering about directions, and therefore with the same number of records, we can repeat the previous procedure, with the input to the local model being represented by H_s, T_m, θ_m (PAR SWAN in the figure). Corresponding time series and statistical distribution are derived (T.S. and "TS A", case B).

On a further reduction of the information, we can have available offshore (at N3) only the statistical distribution of H_s, T_m, θ_m (this must be three-dimensional; two- or one-dimensional ones are of little use). In this case, using the parametric input to Swan, we transfer to the coast every single combination of the parameters, and derive the statistics A at this location, as for the case B. We do not discuss here the latter procedure in details, but we point out that, for a correct evaluation at the coast, the three-dimensional probability space must be suitably modified according to the transformation to which each triplet (H_s, T_m, θ_m) is subjected during the transfer towards the coast.

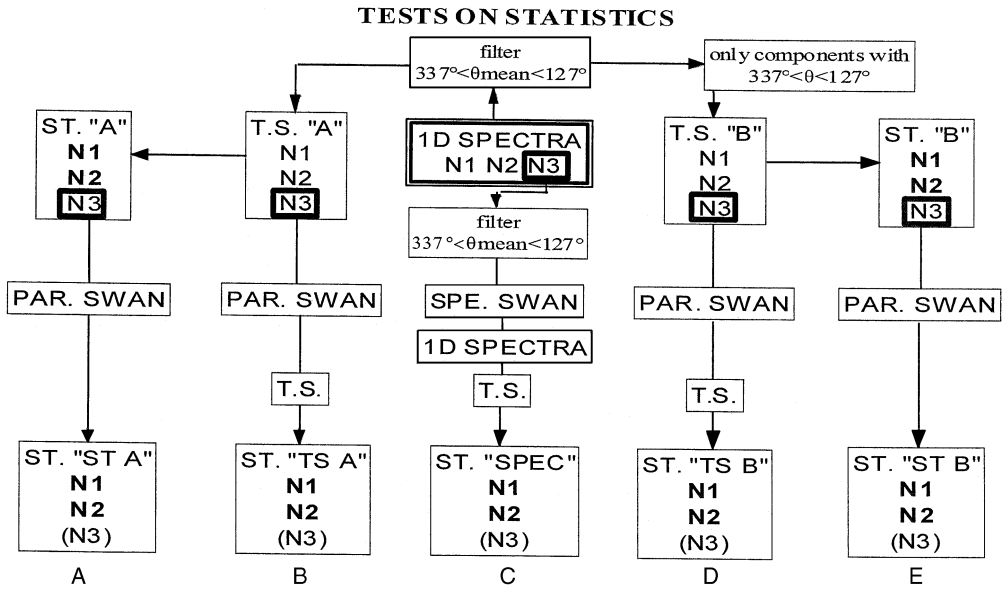

Fig. 6. – Possible approaches to the evaluation of the wave statistics at a coastal location (N1, N2), starting from offshore data at N3. T.S. are time series, ST. is statistics. Filtering on direction is referred to the data from the Holderness campaign; see fig.1 for the locations.

The question is how much the three final distribution C, B, A differ from each other. The positive reply is that they are similar enough to be used (one or the other one) with enough confidence for most of the practical applications. Obviously there is a loss of information passing from C to B and A in fig. 6 (time series of spectra → time series of parameters → statistics), but, if our purpose is the last one, we are in a favourable condition.

There is a limitation to what we have said above. The information given by the triplet H, T, θ does not suffice if we are working in areas, like the open ocean, where we have frequently a superposition of wind sea and swell, most of the time at cross sea conditions. In this case the minimal information for a proper estimate is given by separate triplets, one for each of the two classes of waves.

Going back to the three statistics that we have reported as very similar, as a matter of fact, on a more accurate inspection we do find some differences between the three results. A sensitive parameter is for instance the overall energy E brought by waves to the target location (N1 or N2 in fig. 1). In the case of Holderness we have found $E_A = 1.07E_B = 1.17E_C$, which can be taken, at least in these conditions, as a characteristic result.

The question is where do the differences come from, notwithstanding the use of the same time series as input conditions. There are two reasons for it. The first one, concerning B *vs.* C, is the approximation involved in the spectral representation that Swan devises out of the input triplet H_s, T_m, θ_m. The second one, between A and B, is more subtle. In a discrete statistical distribution each value, *e.g.*, $H_s = 3.0$ m, is taken as representative of all the N cases where H_s is comprised between 2.75 and 3.25 m (here we have assumed an interval $\Delta H_s = 0.5$ m). However, the distribution of the H_s in the interval is typically asymmetrical. Because of the nonlinearities present in the

evolution of the field, this implies that the results from $H_s = 3.0$ m are not representative of those from all the N cases.

In the case of Holderness we have done another test, represented by the results indicated as D and E in fig. 6. Starting from the original input spectra, before passing to parameters and statistics we have retained only the wave components within the selected window (a spectrum with a mean direction within the angular limits can have energy propagating out of them). In a way, for the transfer towards the coast, this is more correct than what done for A and B, when all the components have been retained. In so doing, we obviously lower the wave heights, the amount depending on the mean direction and the directional spreading of the input spectra. While this would be a more sound approach, the kind of data typically available, *i.e.* a triplet of wave parameters, forces the user to consider approaches A and B, for which the above figures, respectively, 1.07 and 1.17, are a typical, but not fixed, reference.

5. – Results from the Montalto di Castro dataset

As we have mentioned in sect. 3, the conditions at Montalto are rather similar to those present at Holderness. In general we do not find here the long swell from the ocean, but this is not essential, because, *mutatis mutandis*, the problem is simply shifted to more shallow waters. Expectably, we have used the same conditions for considering a record, *i.e.* $H_s > 0.5$ m and θ_m within a relatively narrow angle with respect to the perpendicular to the coast.

Having repeated the same tests, we have verified the results previously obtained at Holderness, which are therefore confirmed for this kind of coastal environment, with one notable exception that we now discuss.

5·1. *Bottom friction.* – Following the same layout used for Holderness, fig. 7 shows the results obtained at Montalto with the default option of the Swan model. As in the previous case, there is an overestimate of H_s by the model at the inner buoy. At a first glance the error of 8% could not look too big. However, we must be very careful and look to the data from the correct perspective.

The direct comparison between modelled and measured H_s at the inner buoy, as done in the previous figures, can be misleading. After all, moving the inner buoy closer and closer to the one offshore would apparently improve the results, as all the wave heights would converge to the output value. While this can still be an effective method if used, as we have done, in a differential mode, it can hide the relevance of the process. Starting from given conditions, *i.e.*, a given H_s, at the border of the local grid, our task is to model correctly the changes that take place in time and space. Our model is a good model if it reproduces well these changes. So, for a more through validation, what we need to compare in the scatter diagram is the modelled differences in wave height between the two buoys versus the corresponding measured value.

Once we do so in fig. 8, the results change dramatically. The model succeeds in reproducing more or less only half of the change, and this gives a fair idea of the approximations involved. Note that this diagram has a much more general value than the previous ones, because, within a certain extent, the slope of the best-fit line does not depend on the distance between the two buoys.

A corresponding exercise at Holderness (see the previous section) with the default version of the model showed that there we succeed in justifying 65% of the change. At

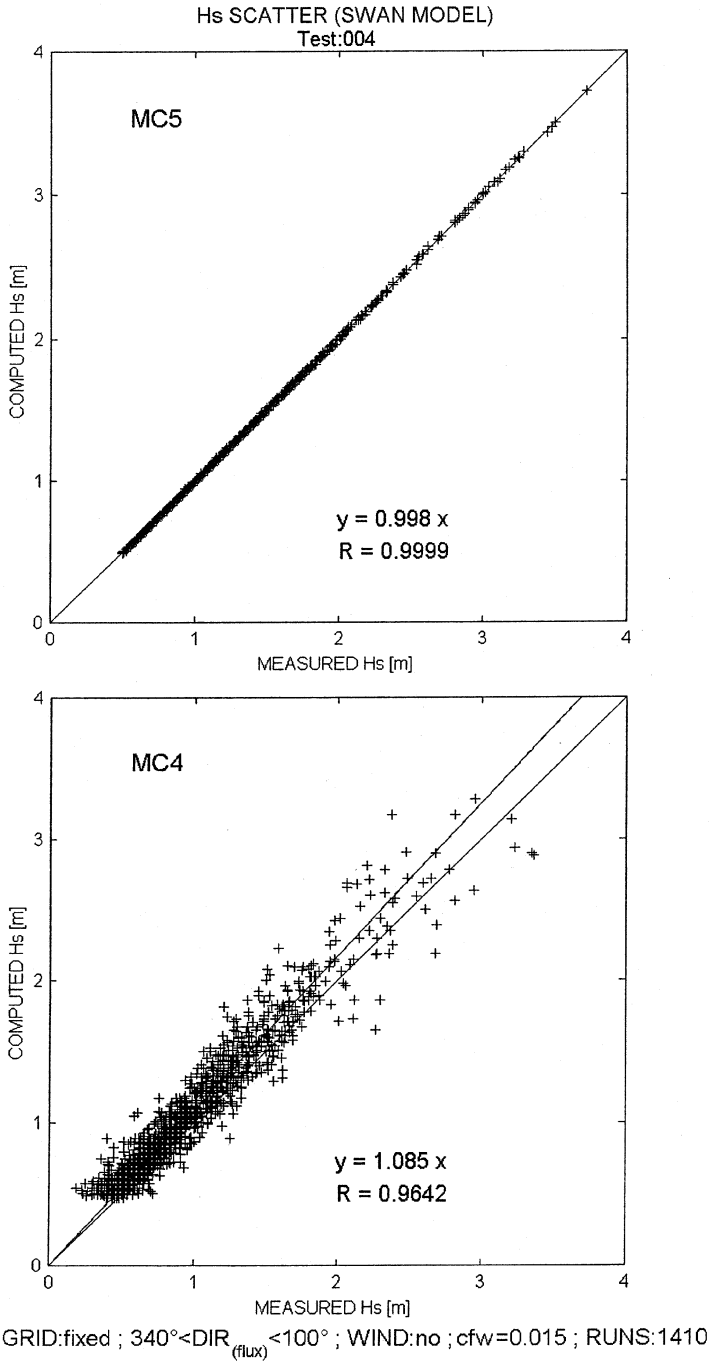

Fig. 7. – Comparison at Montalto di Castro (see fig. 2 for its position) between modelled and measured wave heights at the outer and inner buoys, respectively. The upper line shows the best-fit to the data.

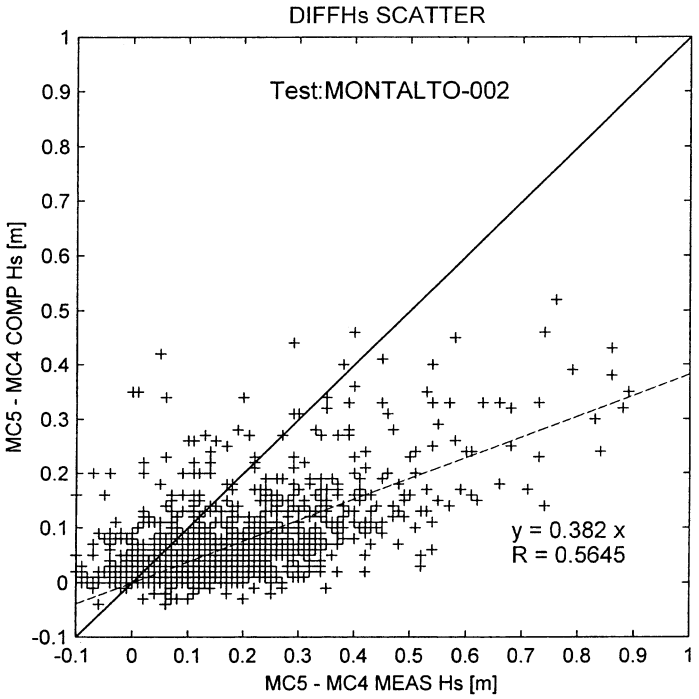

Fig. 8. – Comparison at Montalto di Castro (see fig. 2 for its position) of the modelled wave height differences between the outer and inner buoys *vs.* the corresponding measured value.

Holderness the explanation was associated to the coarse sand, hence to the need to increase the bottom friction coefficient, and therefore the dissipation. However, the sand at Montalto is quite fine, and we were quite puzzled and worried by the results. The explanation, as we discovered later, is associated to the prairie of Posidonia that characterizes the bottom in front of Montalto di Castro. Clearly the large sea-weed, waving with the wave orbital motion, have a much larger attenuation effect on the waves than a sandy bottom, and this fully justifies the results in fig. 8. This is a clear example of how, while setting a model for a coastal zone, it is necessary to obtain proper and complete information on the characteristics of the area. Unluckily, in the case of Montalto the bad news is that, to our knowledge, there is no general theory to evaluate the dissipation of wave energy by Posidonia or similar vegetation. Tryly enough, studies on the hydrodynamic behaviour within the vegetation do exist (see, *e.g.*, Wallace and Cox, 1999), but they have not yet produced a usable summarizing formula or theory. Besides, it is our opinion that the conditions can vary so much, because of size, density, thickness, rigidity of the plants, that it is at least problematic to formulate correctly the loss in quantitative terms. For a given location the only viable solution for accurate results is a measurement campaign to derive empirical coefficients and a sufficient tuning of this part of the model.

5·2. *Geometry of the grid.* – It is correct to wonder if and how much the results of a local model depend on the geometry of the grid. We can vary its extent, resolution,

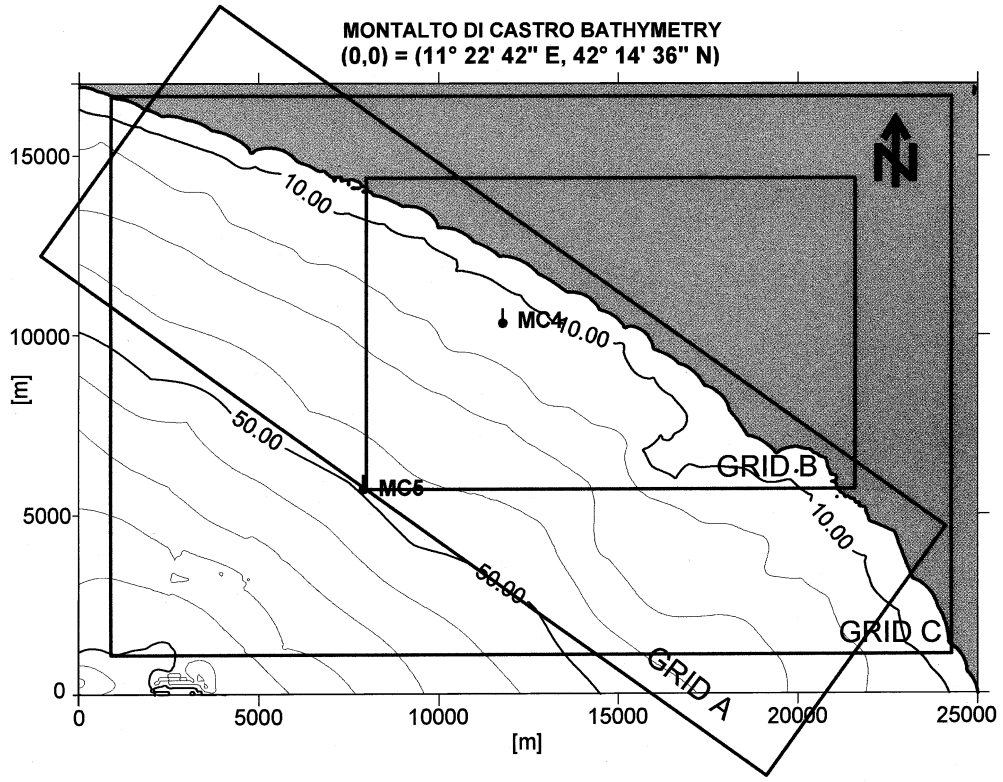

Fig. 9. – The set of grids used for the tests at Montalto di Castro.

orientation, position with respect, *e.g.*, to the location of interest. All this does affect the results; the question is to which extent and if this is relevant for our purposes.

To clarify this point we have carried out a series of specific tests at Montalto di Castro, using the set of grids shown in fig. 9.

As we have already pointed out, with a straight piece of coast the obvious solution is grid A, *i.e.* a rectangular grid, with the longer side parallel to the coast, and the outer border passing through the position where we have the offshore information, in this case the outer buoy. Typically, at least for limited extents, the offshore boundary conditions can be assumed to be uniform along the outer border. For larger grids, if more than one point of information is available, at intermediate points an interpolation can be used.

If the grid is long enough, and hence we assume that no energy from the borders can reach the zone of interest, a no energy input condition can be assumed there. However, we can be interested in saving computer time, hence in keeping the grid as small as possible. In this case a boundary condition must be introduced also at the borders.

The choice of the boundary conditions is really the crucial matter for the choice of the grid. As far as the accuracy of the numerics is concerned, there is hardly any difference among the possible approaches in fig. 9. However, the crucial problem, for instance for the "geographical" grids B and C (borders along latitude and longitude

directions), is which input we should use along their borders. Such grid may be required for a rather wavy coast.

A uniform input, equal to the value present at the reference point MC5, is clearly not realistic, because the wave conditions do change approaching the coast. Also a linear trend with null value at the coast seems too crude (the wave height does not vary in this way). In the case of Montalto the best results were obtained by linearly varying the wave height along the border, consistently with the values measured at the two buoys. This was also the most effective solution in terms of grid extent and computer time. However, this is not the case in most of the practical applications, and some ingenuity is required. A viable solution is to have a first, rather approximate, run to obtain an estimate of how the wave height varies towards the coast. We can then use this result to derive the boundary conditions for the final run. However, we must remember that there is always a degree of approximation.

Whichever grid we set up, it will always be discrete, *i.e.* the results are available only at the knots of the grid. If we are interested on a specific spot, it is natural to try and have it coincident with one of the knots. However, this is not always possible, and it is then correct to wonder how much the necessary interpolation affects the accuracy of our results. To test this, we have shifted (see fig. 9) our geographical grid of half a grid step, and compared the results at the inner buoy. The result was encouraging, as there was hardly any difference. As a matter of fact, the explanation is connencted to the spatial gradients present in the area of interest. If really strong gradients are present, then we need to increse the resolution. Otherwise, the results will be approximate anyway, independently of minor shifts of the grid.

6. – Discussion

We have verified the accuracy and the sensitivity of the results obtained while transfering towards the coast with an advanced third generation wave model wave conditions measured offshore. The analysis of the results has been done on a differential basis and in absolute terms, using the data available closer to shore.

In the considered cases, *i.e.* for comparison at depths not less than ten metres, the results indicate that the dominant factor in determining the inner wave conditions is bottom friction. Generation by wind is negligible on the relatively short distances considered (order of 10 or 20 km), particularly because we have focused our attention on the cases when some energy was present offshore. If wind waves are only locally generated, typically by sea breeze, they are of little interest for most of practical purposes. On the relatively short distances considered, also nonlinear wave-wave interactions turn out to have little effect on the final results.

Conditions would be different in shallower water. Here the dominant role is taken by 3rd-order nonlinear interactions and bottom induced breaking. This has been proven by previous experiments (see Sclavo *et al.*, 1996). Unluckily, we did not succeed in finding a data set with more than one buoy at work on the same location, the inner one being in very shallow water (order of a few metres). Therefore in this range our argumemts are only speculative, based on sound physical principles, but without a quantitative verification.

The shape and dimension of the local grid turned out not to be relevant for the accuracy of the results. However, the key factor is the definition of the boundary conditions at the border of the grid approaching the shore. A viable solution is a

preliminary run, possibly with a coarser grid, providing an approximate information on how the wave conditions change while approaching the shore, then choosing the boundary conditions accordingly.

If the target location is in the area dominated by bottom friction, it is essential to have sufficient information on the characteristics of the bottom. This will then allow the proper choice of the drag coefficient. However, in cases like Montalto di Castro, where the bottom is covered by sea weeds, the only viable solution to have accurate results seems to be a local measurement campaign, aimed at the calibration of the model.

* * *

This paper has been produced under the Mast project *Eurowaves*, MAS3-CT97-0109.

REFERENCES

BOOIJ N., RIS R. C. and HOLTHUIJSEN L. H., *A third-generation wave model for coastal regions - 1. Model description and validation, J. Geophys. Res.*, **104** (1999) 7649-7666.

COLLINS J. I., *Prediction of shallow water spectra, J. Geophys. Res.*, **77** (1972) 2693-2707.

HOLTHUIJSEN L. H., BOOIJ N. and RIS R. C., *A spectral wave model for the coastal zone, Proceedings of the 2nd International Symposium on Ocean Wave Measurement and Analysis, New Orleans, Louisiana, July 25-28, 1993*, pp. 630-641.

KOMEN G. J., CAVALERI L., DONELAN M., HASSELMANN K., HASSELMANN S. and JANSSEN P. A. E. M., *Dynamics and Modelling of Ocean Waves* (Cambridge University Press) 1994, 532 pp.

PRANDLE D., HARRISON A., HUMPHREY J., HOLDAWAY G., LANE A., PLAYER R., WILLIAMS J. J. and WOLF J., *The Holderness Coastal Experiment '93-'96*, POL Report 44, 1996, 48 pp.

RIS R. C., BOOIJ N. and HOLTHUIJSEN L. H., *A third-generation wave model for coastal regions - Part II, verification, J. Geophys. Res.*, **104** (1999) 7667-7681.

SCLAVO M. and CAVALERI L., *Sensitivity analysis on the transfer of the offshore conditions to a coastal location, ISOPE-99, Brest, France, 30 May - 4 June 1999.*

SCLAVO M., LIBERATORE G. and RIDOLFO R., *Waves in front of the Venetian littoral, Nuovo Cimento C*, **19** (1996) 125-150.

SLEATH J. F. A., *Sea Bed Mechanics* (John Wiley & Sons, New York) 335 pp.

WALLACE S. and COX R., *Flow propagation over seagrass meadows and the implications for coastal waters, Proceedings of the Fifth International Conference Coastal and Port Engineering in Developing Countries, pp. 49-58, Copedec, Cape Town, S. Africa, 19-23 April 1999*, 2253 pp.